

Petrology, Geochemistry and Tectonomagmatic Setting of Neshveh Intrusion (NW Saveh)

Reza Keshavarzi¹, Dariush Esmaili¹, Mehdi Rezaei Kahkhaei¹, Mir Ali Asghar Mokhtari^{2*}, Reza Jabari³

¹School of Geology, Faculty of Science, University of Tehran, Tehran, Iran

²Geology Group, Faculty of Science, University of Zanjan, Zanjan, Iran

³Geology group, Faculty of Science, Islamic Azad University of Science and Research of Tehran, Tehran, Iran
Email: amokhtari@znu.ac.ir

Received 17 February 2014; revised 15 March 2014; accepted 22 March 2014

Copyright © 2014 by authors and Scientific Research Publishing Inc.

This work is licensed under the Creative Commons Attribution International License (CC BY).

<http://creativecommons.org/licenses/by/4.0/>



Open Access

Abstract

Neshveh intrusion is located in the NW of Saveh City and is a part of Orumieh-Dokhtar magmatic arc. This intrusion consists of quartz monzodiorite, granodiorite and granite that have intruded into the Eocene volcano-sedimentary rocks. This intrusion is high-K calc-alkaline and metaluminous and is classified as I-type granitoids. Field investigations along with petrographic and geochemical studies indicate that all phases of Neshveh intrusion are derived from a common magma source as a result of mineral differentiation. Different phases of this intrusion have low Mg#, Ni, Cr, Co and V which are indicative for higher evolution of magma during the magma ascent and before complete crystallization. All phases of Neshveh granitoid are characterized by LREE-rich patterns with high LREE/HREE ratio and negative Eu anomalies. Similarity of the mentioned patterns suggests a comagmatic source for these rocks and demonstrates the role of magmatic differentiation in their evolution. There are negative anomalies in the Nb and Ti along with positive anomalies of Rb, Ba, K and Pb on the spider diagrams. These anomalies are indicative for a subduction setting for magma source of these rocks. Geochemical studies indicate that the Neshveh granitoid is formed in a volcanic arc and active continental margin. In this base, it is assumed that this intrusion is formed as a result of Neo-Tethys oceanic lithosphere subduction beneath the Central Iran zone which is replaced in the Orumieh-Dokhtar magmatic arc.

Keywords

Petrology, Geochemistry, Intrusion, Granitoid, Neshveh, Saveh

*Corresponding author.

1. Introduction

Neshveh intrusion is located in the north west of Saveh and is a small part of the Orumieh-Dokhtar magmatic arc in the Alpine-Himalayan orogenic belt. Volcanic rocks are so common in the Orumieh-Dokhtar magmatic arc. These rocks have varieties in composition and tectonic setting which are varying from acidic to basic and continental to shallow marine environments. There are some intrusions also within the volcanic rocks. Acidic-intermediate volcanic and intrusive rocks are widespread in contrast to basic rocks that are probably indicative for the effect of continental crust in their formation.

Several studies had been carried out in the Saveh region, such as studies of [1] and [2] which were focused on the petrography and Petrochemistry of igneous rocks in the south west of Saveh, volcanic and plutonic rocks in the south of studied area. According to [3], volcanic rocks around the Neshveh village consist of three parts: the oldest volcanic rocks include rhyolite, dacite and some andesite; pyroclastic rocks and lava flows along with intercalation of marl, sandstone and limestone with Lutetian age; and finally andesites and latites with porphyritic textures in the upper part with Priabonian age. The Eocene volcanic flows are widespread in the studied area, which are the result of hybrid crustal-mantle source. The hybrid source of these rocks is attributed to the ascending of basic magma with mantlic source and melting of the continental crust.

Neshveh intrusion located between $35^{\circ}10'$ to $35^{\circ}14'$ latitudes and $50^{\circ}10'$ to $50^{\circ}14'$ longitude at the 40 km north west of Saveh. This intrusion was intruded into the volcanic-sedimentary rocks of Eocene (Figure 1). This intrusion didn't investigate for detail petrology and geochemistry, yet. Also, no reliable analyses of trace elements have been published from this intrusion. This research is a detailed study on the petrology and geochemistry of major and trace elements and tectonomagmatic setting of the Neshveh intrusion.

2. Geology

Neshveh region which is located in the north west of Saveh is a small part of the Orumieh-Dokhtar magmatic arc within the Central Iran zone. All rocks crops out in this region have Cenozoic age and older rocks don't exposed. Based on Saveh geological map 1:100,000 [4], the main rocks in this area consist of sedimentary, volcanic and intrusive rocks have Paleocene-Eocene age and later (Figure 2). These rocks composed of conglomerate equal to Fajan formation, volcanic-sedimentary rocks of Middle-Upper Eocene consist of intermediate-acidic tuffs and lavas, agglomerate and intermediate-basic lavas along with the tuffaceous and sandy limestone and finally Upper Eocene ignimbrite, Lower Red Formation (conglomerate, sandstone, siltstone and red-brown marl), Qom Formation (limestone, marly limestone and marl), Upper Red Formation (conglomerate with red sandstone intercalation), Mio-Pliocene marl, conglomerate equal to Hezar Dareh Formation and quaternary alluvial deposits.

Several granitoid intrusions were intruded into the Eocene volcanic-sedimentary rocks. Dating of some of these intrusions by [1] by K-Ar method on the amphibole, biotite, K-feldspar and whole rock indicate 28 - 42 Ma

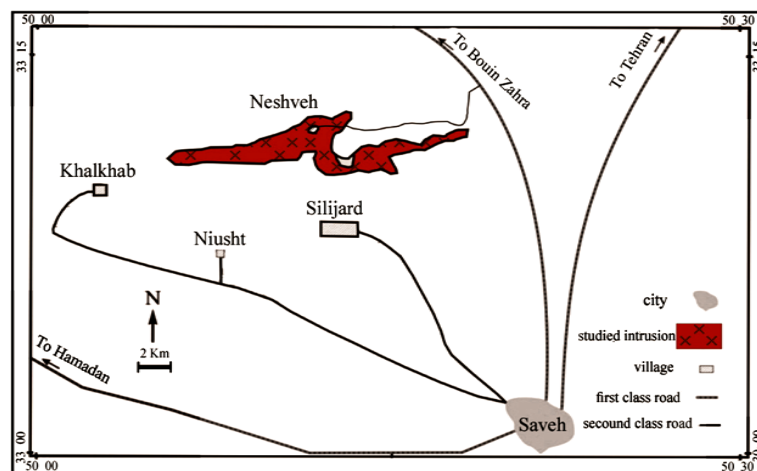


Figure 1. Geographic location of the Neshveh intrusion in the northwest Saveh.

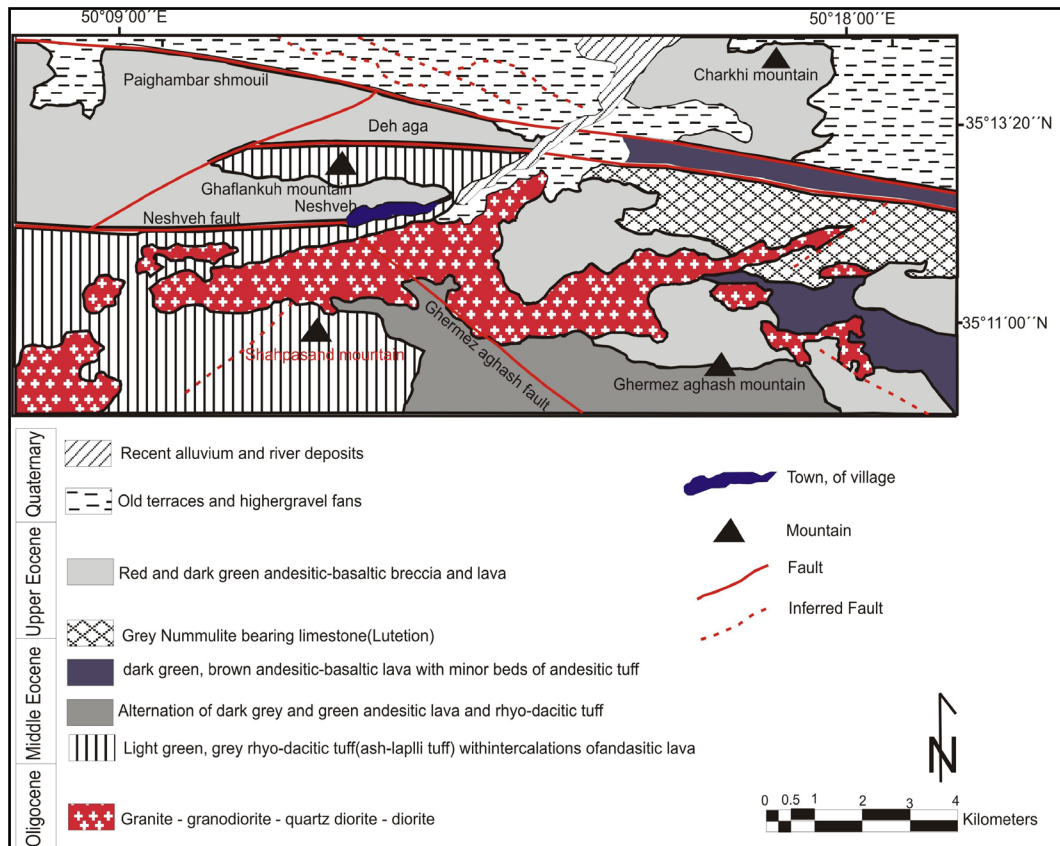


Figure 2. The geological map of studied area based on 1:100,000 geological map of Saveh [4].

(Table 1). The Silijard granite, Kalkhab tonalite-diorite, Neshveh granitoid (this study) and Niousht micro-granite are the most important intrusions in the northwest of Saveh.

In addition to mentioned intrusives, some sub-volcanic domes also exist in different parts of the northwest Saveh that have acidic-intermediate composition. These domes intruded into the Upper Eocene-Oligocene intrusives. In this base, these sub-volcanic intrusions attributed to the Post Oligocene.

There are some acidic and basic dykes in this area. Basic dykes with andesite-andesitic basalt composition are widespread in comparison to acidic dike with dacite-andesite composition. These dikes cut the Eocene volcanic rocks and Oligocene intrusives. In this base, their intrusions have been attributed to the post Oligocene.

3. Research Methods

Our researches in this study consist of two parts: field and laboratory studies. Field studies include identifying the different phases of intrusion, relationship between them and host rock and finally sampling of different phases for laboratory studies. Laboratory investigations include preparing of 90 thin section and petrographic studies, analyzing of 9 samples by ICP-AES and ICP-MS for major, trace and rare earth elements at the ALS Chemex (Table 2). Finally, these analyses were processed by using Excel, Minpet, GCDKit and Iqpet programs.

4. Petrography

Neshveh granitic intrusion with an area about 22 km², consist of intrusive rocks in the mountains of Shahpasand and Zarou, north of Jafarabad Village, north of Aftabroo Qeshlaq village and south of Neshveh village. This intrusion crops out in the east-west trend and intruded into the Upper Eocene volcanic-sedimentary rocks (Figure 3). There are chloritic and argillic alterations present at the contact of intrusion with host rocks. Major faults include Kooshk Nosrat, Neshveh and QermezAghaj with NW-SE trend cut the Neshveh granitic intrusion and caused to crushing and fracturing the intrusion (Figure 3). Moreover, this intrusion cut by a series of andesitic-

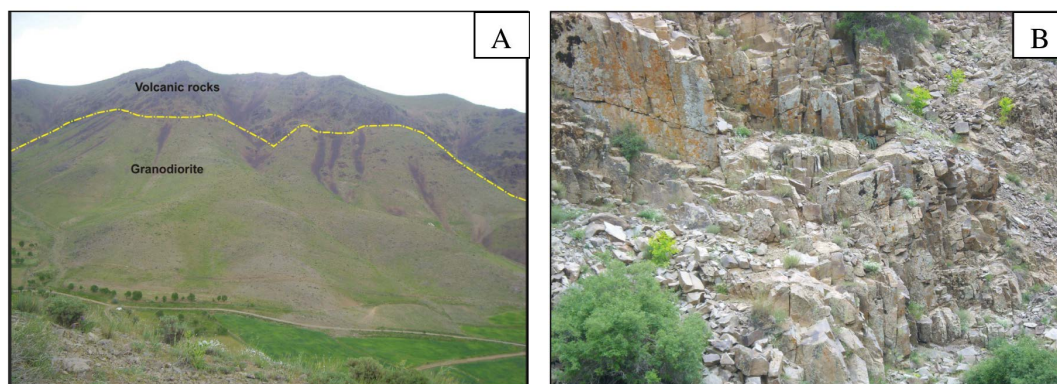


Figure 3. (a) View from the Neshveh intrusion and its contact with Eocene volcanic-sedimentary rocks (view to the south); (b) Close view from the fracturing in the Neshveh intrusion as a result of tectonic.

Table 1. The result of dating analysis on the some intrusions around the Saveh [1].

Biotites	37 - 41 Ma
Amphiboles	31 - 38 Ma
Alkali Feldspars	35 - 42 Ma
Whole rocks	28 - 39 Ma

basaltic dikes. Some xenoliths of the Eocene volcanic rocks present at the marginal parts of the intrusion, which their dimension and frequency decrease to the interior part. In addition, there are some mafic micro-granular enclaves in different parts of the Neshveh intrusion which are characterized by rounded shapes. These enclaves mineralogically composed of the monzodiorite and diorite.

Based on Petrographic studies of 90 samples from different parts of the Neshveh intrusion, it was subdivided into two compositional zones: quartz monzogabbro in the West and quartz monzodiorite, granodiorite and granite in the East (**Figure 4**). The contacts are gradational but the rock types are distinct and easily recognized both in outcrop and in aerial photos and satellite images. Compositionally, dikes include andesite-basaltic andesite. Samples Neshveh intrusion has medium to coarse grained granular texture which is locally accompanied by porphyroidic texture with plagioclase phenocrysts, micro-granular and graphic texture.

The quartz monzogabbro occupies about 50% of the pluton and is medium to coarse-grained with various textures; some samples show inter-granular and poikilitic textures, while others show hetero-granular texture. The inter-granular texture is constituted by grains of clinopyroxene which occupy the angular interstices between plagioclase crystals. The quartz monzogabbro consists dominantly of plagioclase (51.5 - 55.6 modal %), clinopyroxene (20.2% - 25.7%), K-feldspar (9% - 14.1%), quartz (7.9% - 11.7%), and subordinate opaque minerals (2.3% - 3.5%) and apatite (0.6%).

The quartz monzodiorite surrounds the granodiorite and granite. To the west, quartz monzodiorite is transitional to more mafic rocks, the quartz monzogabbro while to the east it forms the margin of the pluton. The quartz monzodiorite is generally medium-grained and characterized by equi-granular texture. It consists dominantly of plagioclase (41.1% - 52.4 modal %), K-feldspar (9% - 19%), quartz (10.9% - 18.4%), hornblende (6.9% - 16.3%), subordinates clinopyroxene (0% - 12.1%), biotite (2.5% - 5%) and opaque minerals (2.3% - 3%) (**Table 1**). Accessory minerals such as titanite and apatite are rare.

About 20% of the Neshveh intrusion is constituted by granodiorite, emplaced within the quartz monzodiorite hosted by volcanic rocks. These rocks are mainly included plagioclase (40% - 45%), quartz (approximately 20%), alkali feldspar (15% - 20%), hornblende (~10%) and biotite (~5%). Granites are the next order and generally emplaced at the eastern part of the intrusion. These rocks are predominantly of medium-grained granular texture, but porphyroidic texture with plagioclase phenocrysts present also. Granites composed of plagioclase (35% - 40%), quartz (~25%), alkali feldspar (~30%), hornblende (~5%) and biotite (~1%).

In the all type of rocks at the studied area, plagioclase present as euhedral and subhedral crystals and are of andesine and oligoclase type. Some of them show zoning (**Figure 5**). These minerals underwent low grade alte-

Table 2. The result of samples analysis from the studied area by ICP-AES and ICP-MS methods (major elements in % and trace elements in ppm).

Rock Type	<u>Andesitic Basalt</u>		<u>Granodiorite</u>			<u>Granite</u>		<u>Qz Monzodiorite</u>	
Sample No.	SN05	SN15	SN17	SN31	SN48	SN44	SN52	SN10	SN11
SiO ₂	49	62.7	62.5	62.3	64	65.1	69.4	56.5	59.6
TiO ₂	1.12	0.57	0.51	0.59	0.53	0.49	0.32	0.73	0.71
Al ₂ O ₃	14.65	16.15	15.45	15.75	15.65	14.8	13.8	17.1	16.7
Fe ₂ O ₃	13.4	6.03	5.07	5.98	5.17	3.89	3.05	8.66	7.66
MnO	0.22	0.15	0.13	0.1	0.09	0.05	0.07	0.14	0.14
MgO	5.09	1.78	2.05	2.58	1.98	1.52	1.1	3.26	2.48
CaO	7.89	4.81	3.38	4.15	3.8	4.84	2.27	7.16	5.89
Na ₂ O	4.28	3.49	3.64	3.36	3.41	3.47	3.06	3.23	3.59
K ₂ O	1.14	2.73	3.46	2.95	3.26	2.9	4.19	1.85	2.31
P ₂ O ₅	0.15	0.19	0.15	0.19	0.16	0.15	0.09	0.23	0.2
Total	96.94	98.6	96.34	97.95	98.05	97.21	97.35	98.86	99.28
V	506	128	89	118	87	76	47	241	194
Cr	15.9	10	10	10	10	10	10	20	10
Ni	19	8	5	6	5	5	5	14	8
Co	15	12.8	8	12	10.2	5	4	23.8	17.4
Cu	19	47	22	59	17	5	8	53	48
Zn	98	76	80	40	51	23	44	51	75
Ga	17.6	16.2	15	15.3	15.3	14.4	13.2	17.5	17.7
Sn	8	1	1	1	1	2	1	2	1
W	1	2	2	2	2	1	1	1	2
Ba	354	675	701	618	665	759	808	465	548
Sr	271	449	347	381	352	353	248	503	424
Rb	29.5	71.4	74.2	63.5	78.2	38.1	90.8	48.7	60.9
Nb	1.5	6.6	7.9	6.5	8.2	7.4	8.7	4.8	6.6
Y	22	20.4	21.6	17.5	19.7	18.4	16.2	20.9	23
Zr	81	121	134	113	145	145	124	83	119
Cs	0.71	1.22	1.49	1.19	1.74	0.4	1.47	1.95	2.34
Hf	2.3	3.6	3.8	3.1	4.1	4.1	3.8	2.4	3.5
Ta	0.1	0.5	0.5	0.5	0.5	0.5	0.7	0.3	0.5
Th	0.35	5.55	5.89	4.98	6.18	5.91	8.42	3.17	5.11
U	1.87	1.43	1.3	1.05	0.97	1.56	1.78	0.71	1.23
La	23.2	24.2	16.8	13.1	13.1	16	19.7	14	15.3
Ce	39.5	45.7	32.6	25.6	26.6	31.6	34.9	28.4	30.8
Pr	3.93	5.24	4.07	3.3	3.53	3.85	3.9	3.64	3.85

Continued

Nd	13.2	19.3	16.2	13.3	14.2	14.9	14.2	14.9	15.4
Sm	2.9	3.76	3.7	3.1	3.43	3.21	2.84	3.38	3.53
Eu	1.53	0.95	0.91	0.98	0.9	0.88	0.6	0.99	0.94
Gd	3.77	3.91	4.15	3.4	3.69	3.65	2.99	3.67	3.87
Tb	0.62	0.56	0.64	0.54	0.59	0.55	0.46	0.59	0.62
Dy	4.14	3.48	3.88	3.22	3.56	3.26	2.8	3.73	4
Ho	0.83	0.71	0.83	0.66	0.74	0.69	0.6	0.77	0.8
Er	2.53	2.12	2.41	1.99	2.28	2.12	1.89	2.18	2.45
Tm	0.36	0.32	0.37	0.29	0.34	0.32	0.29	0.32	0.34
Yb	2.37	2.14	2.44	1.93	2.29	2.16	2.06	2.24	2.39
Lu	0.39	0.36	0.37	0.29	0.36	0.33	0.34	0.33	0.4
Mo	2	2	2	2	2	2	2	2	2
Pb	0.5	13	21	10	15	6	17	7	11
Tl	0.5	0.5	0.5	0.5	0.5	0.5	0.5	0.5	0.5

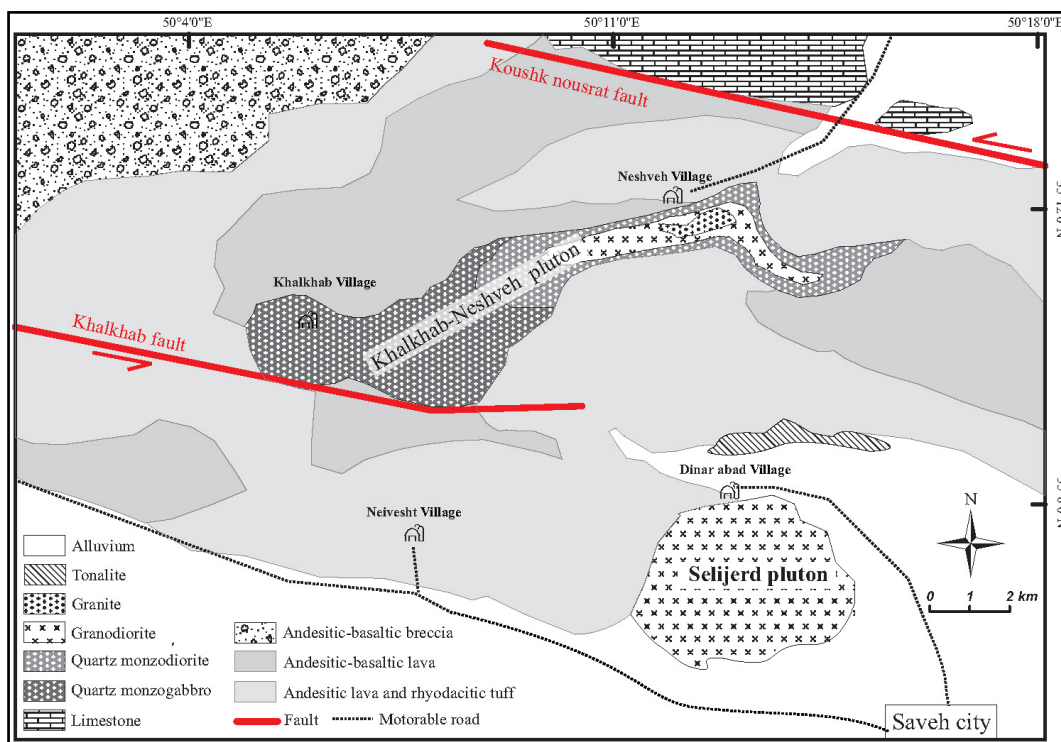


Figure 4. Simplified geological map of NW Saveh intrusions (Based on satellite data and the geological map of Saveh in 1:100,000 scale; Galamgash and Fonudi, 1998).

ration to sericite and sometimes epidote and calcite (Figure 5). Alkali feldspars (orthoclase) indicate argillic alteration in some samples. At the granitic samples, perthite texture was formed as a result of sub-solidus processes. Quartz presents as fine to medium-grained xenomorphic crystals between the other minerals. Graphic texture was formed as a result of quartz and orthoclase in the granites and occasionally in granodiorites (Figure 5). In some samples, quartz shows wavy extinction indicating tectonic stresses on the intrusion. Mafic minerals

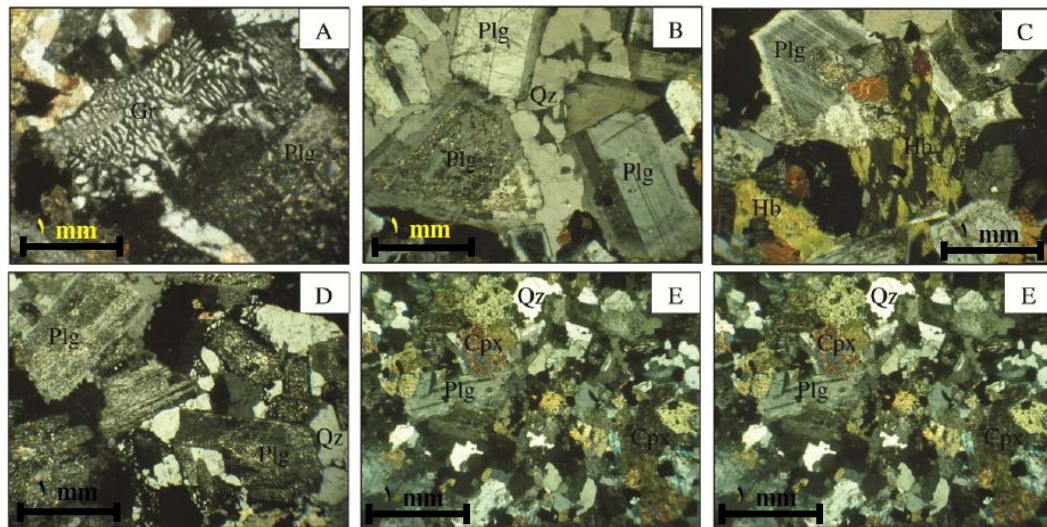


Figure 5. (A) Graphic texture in the granites and granodiorites (XPL light); (B) Plagioclase crystal that underwent epidote, sericite and chlorite alteration from the center (XPL light); (C) A plagioclase with zoning (XPL light); (D) Sericitized plagioclase crystals (XPL light); (E) Clinopyroxene bearing microgranular texture in the quartz-monzodiorite (XPL light); (F) Porphyritic texture includes plagioclase phenocrysts within the plagioclase, amphibole and pyroxene bearing fine-grained matrix (XPL light). (Gr: graphic, Plg: plagioclase, Qz: quartz, Hb: hornblende, Cpx: clinopyroxene).

in the Neshveh intrusion are mainly hornblende and biotite is less. Hornblende present as euhedral and subhedral crystals at the all phases of Neshveh intrusion (**Figure 5**). Some crystals of hornblende, altered to actinolite which sometimes accompanied by biotite and iron hydroxides. Biotite present at the all phases of this intrusion which its content increase at the granites. Clinopyroxene is observed with low frequency in the quartz-monzodiorite which mainly has been replaced by actinolite. The rests of the clinopyroxene are found as islands form within the actinolite (**Figure 5**). Sphene, opaque, zircon and apatite are the minor minerals in the Neshveh intrusion and secondary minerals include sericite, epidote, actinolite, chlorite and clay minerals.

As mentioned before, there are some medium-basic dykes within the Neshveh intrusion that compositionally are andesite and basaltic andesite. They have porphyry, microlitic porphyry, inter-granular and intersertal textures phenocrysts of plagioclase, clinopyroxene and hornblende in a fine-grained to microlitic matrix (**Figure 5**). Some plagioclase crystals show zoning and classified as andesine-labradorite. Some plagioclase crystals altered to sericite and some clinopyroxene crystals show alteration to chlorite. Fine-grained matrix underwent alteration to chlorite.

5. Geochemistry

For studying of geochemical characteristics of Neshveh intrusion, 8 samples from plutonic rock and one sample from basaltic andesite dikes were analyzed at the ALS Chemex laboratories for major, trace and rare earth elements by ICP-MS and ICP-AES analysis method. The results of this analysis are presented in **Table 1**.

Based on $K_2O + Na_2O$ versus SiO_2 diagram [5] and [6] and the AFM triangular diagram [5], all rocks units of the Neshveh intrusion are calc-alkaline character (**Figure 6**). At the SiO_2 against K_2O diagram [7], they are classified as high potassium calc-alkaline rocks (**Figure 7**). Based on calcic-alkali index [8], all samples Neshveh intrusion have Calc-alkali nature (**Figure 7**). On the ASI versus A/NK diagram [9], all samples are classified as metaluminous rocks (**Figure 7**). K_2O/Na_2O ratio is more than one in the studied rocks.

Granitic rocks have been classified as M, I, S, A and H-type by some researchers [e.g., [10]-[15]]. Several evidences suggest that the Neshveh intrusion is I-type and possibly Andean type: 1-Frequency of hornblende, magnetite, biotite and titanite in these rocks and absence of muscovite, garnet, cordierite, andalusite and sillimanite. 2- SiO_2 content varies between 56.5% - 69.4% in these rocks. 3-Presence of mafic micro-granular enclaves in different parts of the intrusion and the absence of micaceous xenoliths [16]. 4-Absence of normative corundum in the samples and metaluminous nature of them. 5-Absence of pegmatites. 6-Decreasing P_2O_5 versus

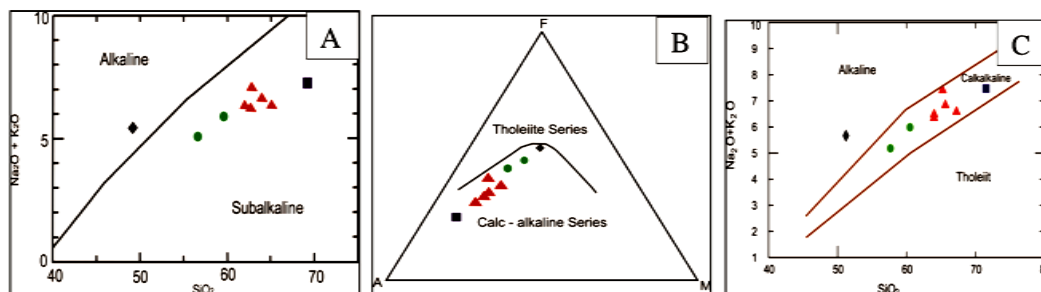


Figure 6. Location of the samples from studied area on the: (A) SiO_2 versus $\text{Na}_2\text{O}+\text{K}_2\text{O}$ diagram [5], (B) AFM diagram [5], and (C) SiO_2 versus $\text{Na}_2\text{O}+\text{K}_2\text{O}$ diagram [6].

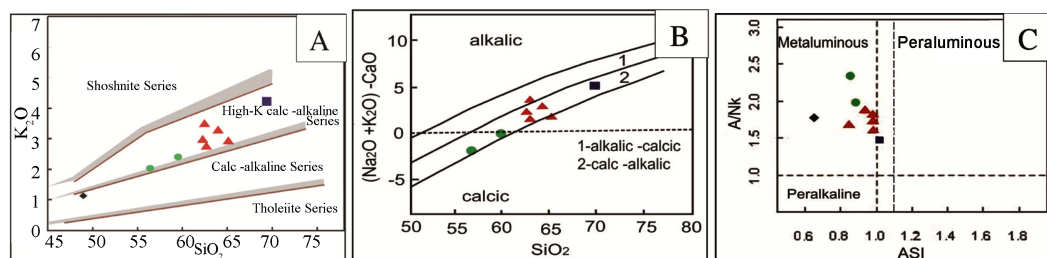


Figure 7. Location of the samples from studied area on the: (A) SiO_2 versus K_2O diagram [7]; (B) SiO_2 versus $(\text{Na}_2\text{O}+\text{K}_2\text{O})-\text{CaO}$ diagram [8], and (C) ASI versus A/NK diagram [9].

SiO_2 [17] (**Figure 8**). 7-Based on SiO_2 vs. K_2O [15] and ACNK versus SiO_2 diagrams [18], the Neshveh intrusion classified as I-type granitoids (**Figure 8**).

[19] classified granitoids into 7 main groups. Based on this classification, Neshveh intrusion is classified as amphibole-bearing calc-alkaline granitoids (ACG).

On the variation diagrams, with increasing SiO_2 , contents of Al_2O_3 , P_2O_5 , CaO , TiO_2 , MgO , MnO and Fe_2O_3 are decreased and K_2O and Na_2O demonstrate increasing trend. These trends may reflect the crystal fractionation process in the evolution of the Neshveh intrusion. The Nd/Sr vs. La/Nb diagram [20], is useful indicator for fractionation of plagioclase in the magma. Based on **Figure 8**, crystallization and fractionation of plagioclase led to increasing of the Nd/Sr ratio in the magma while the La/Nb ratio will be constant.

[21] exhibited a method to recognition of the three main processes of partial melting, fractional crystallization and magma mixing in the magmas. In this method, an incompatible element is used against a consistent element. According to this method, the consistent element put in the horizontal axis and the incompatible element is in the vertical axis. If the trend of samples is a smooth and straight and almost horizontal line, fractional crystallization is the probable process in the magma evolution. If the trend is a smooth and straight and almost vertical line, partial melting is the effective process in the evolution of magma. In the cases that the trends of samples show a concave curved, this trend indicating that the magma mixing is the most probable process in the evolution of magma. In the V vs. Rb and Ba diagrams (**Figure 9**), despite the very small scattering, samples of the Neshveh intrusion has relatively horizontal trend indicating that the main mechanism for evolution of the Neshveh intrusion was the fractional crystallization.

Based on geochemical studies, Neshveh granitoid can be classified as sodic granite ($\text{Na}_2\text{O} > \text{K}_2\text{O}$) and has low values of Mg#, Ni, Cr, Co and V. Lower contents of these elements indicative for evolution of magma during ascending and before complete crystallization [22].

The primitive mantle normalized spider diagrams for different units of Neshveh intrusion demonstrate negative anomalies of HFSEs including Nb, Ti and P, along with positive anomalies in LILEs including Rb, Ba, Th, K and Pb (**Figure 10**). The negative anomalies of Ti and Nb are controlled by titanium bearing minerals such as titanite, ilmenite, rutile, garnet and some amphiboles. With increasing pressure, the solubility of titanium bearing minerals reduces in aqueous fluids [24]. Therefore, these minerals that are rich in HFSEs will be stable during partial melting process at depths greater than 30 km that is led to negative anomalies in the melt [24]. The negative anomaly in P indicative for low content of apatite in the studied rocks. As mentioned before, in the I-type granitoids, phosphorus act as a consistent element and fractionation this element in the early stages of magma-

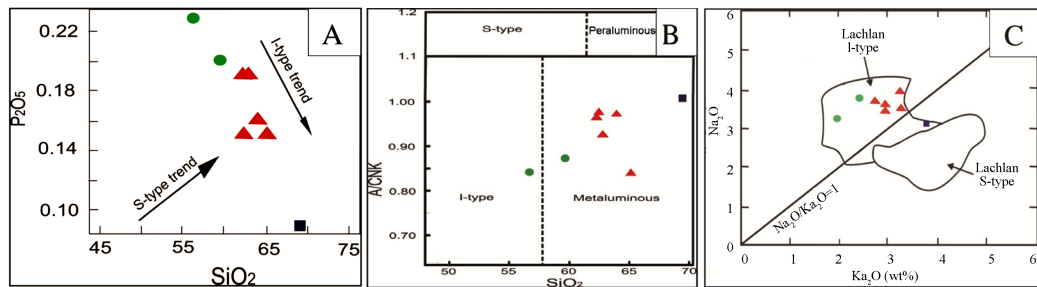


Figure 8. (A) Decreasing trend of P_2O_5 versus SiO_2 [17]. Location of the samples from studied area on the (B) SiO_2 versus A/CNK [18], and (C) SiO_2 versus Na_2O [15].

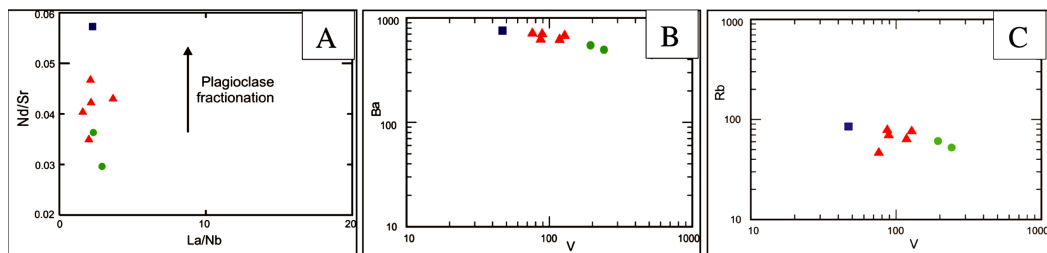


Figure 9. (A) Increasing trend in the Nd/Sr versus La/Nb which is indicative for plagioclase fractionation; (B) and (C) Decreasing trend of Rb and Ba versus V which is indicative for fractional crystallization on the evolution of Neshveh intrusion.

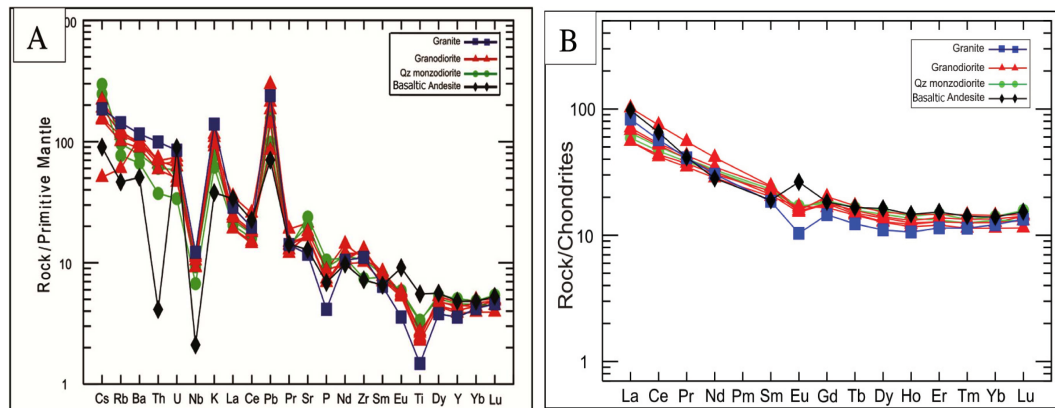


Figure 10. (A) Primitive mantle [23] normalized spider diagram for the studied rocks; (B) Chondrite normalized [23] REE patterns for the studied rocks.

crystallization, led to negative anomalies in the crystallized rocks. The sample from dikes has negative Th anomalies (Figure 9). Based on mineralogical and geochemical composition of dykes; it seems that their parental magma source is the mantle. Since the Th content in the mantle is higher than the crust, this negative anomaly indicating that this magma rise up rapidly and underwent very low crustal contamination.

Fluids and melts derived from the subducted oceanic slab, led to the metasomatism of upper mantle wedge and thereupon, negative anomalies of Nb and Ta [25]-[27]. Positive anomalies in Pb, K, Rb and Ba are attributed to metasomatism of mantle wedge by fluids derived from the subducted slab or/and contamination with continental crust [28] [29].

The Chondrite-normalized REE patterns in the different phases of Neshveh intrusion show a LREE rich pattern with a high LREE/HREE ratio (Figure 10). All phases of Neshveh intrusion indicate negative anomalies Eu while sample from the dikes show a positive anomaly in Eu (Figure 10). Negative anomalies in Eu are related to the feldspar fractionation during magma crystallization or remaining of feldspar at the source. If these negative anomalies are associated with negative anomalies in Sr, fractional crystallization of plagioclase is re-

sponsible for these anomalies. While, the negative anomalies in Eu are associated with negative anomalies in Ba, K-feldspar fractionation has the main role in this respect [25]. In the studied rocks, negative anomalies of Eu occur along with Sr, which refers to the plagioclase fractionation. Positive anomaly in Eu from the dike sample is indicative for the absence of plagioclase fractionation during the magma crystallization and high concentration of this mineral in these rocks.

6. Tectonomagmatic Setting

Besides the geochemical characteristics of rare elements such as spider diagrams, tectonomagmatic setting discrimination diagrams also demonstrate a subduction setting relation for the Neshveh granitoid.

Based on the [30] diagram that is offered with considering, two cationic parameters include $R2 = 6Ca + 2Mg + Al$ and $R1 = 4Si - 11(Na + K) - 2(Fe + Ti)$, samples of Neshveh intrusion put into the pre-plate collision setting (Figure 11). On the [31] triangular diagrams that are drawn based on immobile elements include Ta and Hf and mobile element of Rb, samples of studied intrusion put into the volcanic arc (VA) setting (Figure 11)

Based on the Rb versus $Y + Nb$ and Rb versus $Ta + Yb$ diagrams [32] samples from the Neshveh intrusion put in the volcanic arc granite (VAG) setting (Figure 12). On the Th/Hf versus Ta/Hf, Th/Ta versus Yb and Ta/Yb versus Th/Ta diagrams [33], all samples from the Neshveh intrusion put into the active continental margins are (Figure 13). The sample from the dikes is situated in the within plate setting (Figure 13).

Based on the AFM diagram [34], the studied rocks located in the continental arc granites (CAG) setting (Figure 14), indicating that these granitoids originated from the subduction of an oceanic crust under a continental crust at the active continental margins. The parental magma was medium to high K calc-alkaline.

The Th/Yb versus Ta/Yb diagram [35] was used to recognition the source magma for Neshveh intrusion. According to this diagram, the studied samples are located within the calc-alkaline Andean granitoids (Figure 15). Moreover, the variation trend of samples on this diagram indicates the evolution of magma by fractional crystallization.

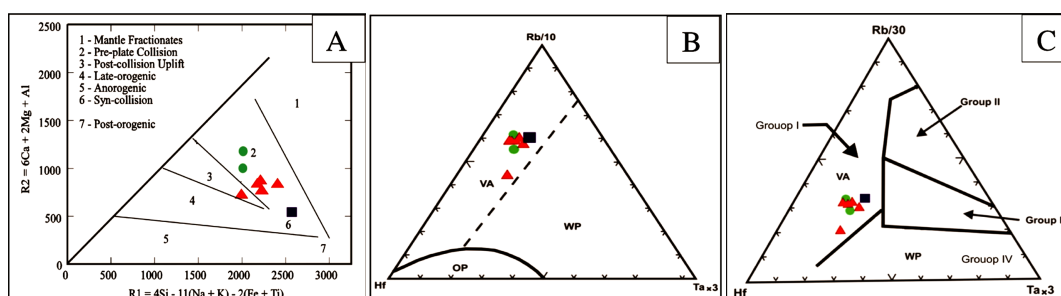


Figure 11. (A) Location of the Neshveh intrusion samples on the two cationic parameters of R1 and R2 [29]. (B) and (C) Location of the Neshveh intrusion samples on the Hf-Ta-Rb triangular diagrams [30].

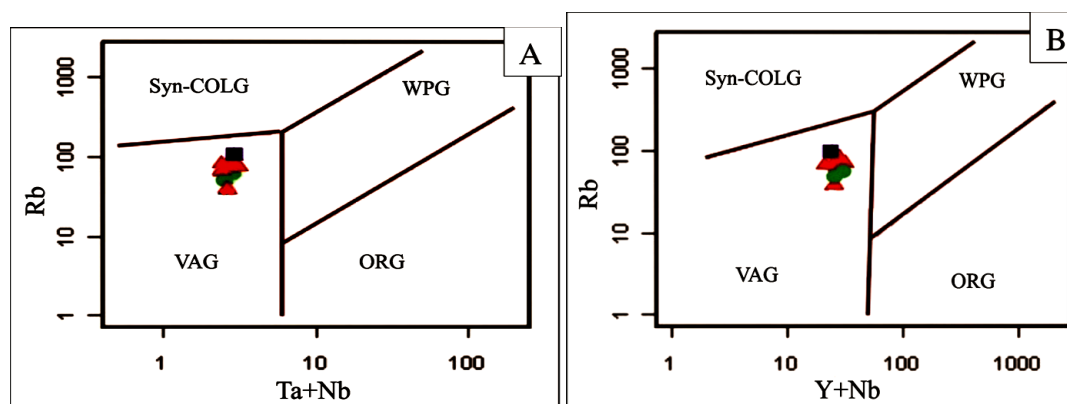


Figure 12. Location of the Studied samples on the: (A) Rb versus $Ta + Yb$ diagram [31]; and (B) Rb versus $Y + Nb$ diagram [31].

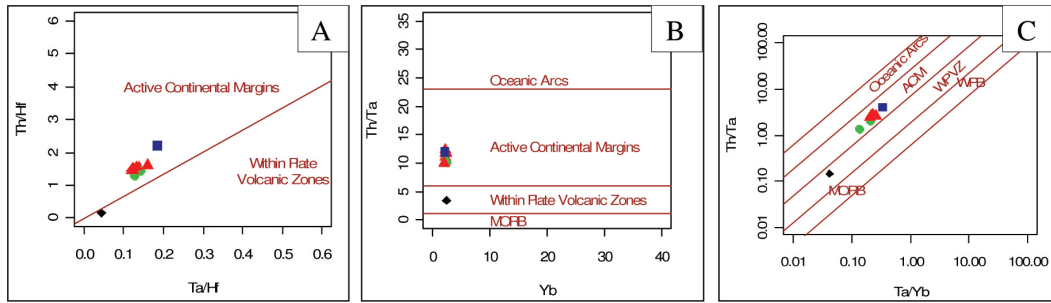


Figure 13. Location of the Studied samples on the: (A) Th/Hf versus Ta/Hf; (B) Yb versus Th/Ta; and (C) Th/Ta versus Ta/Yb diagrams [32].

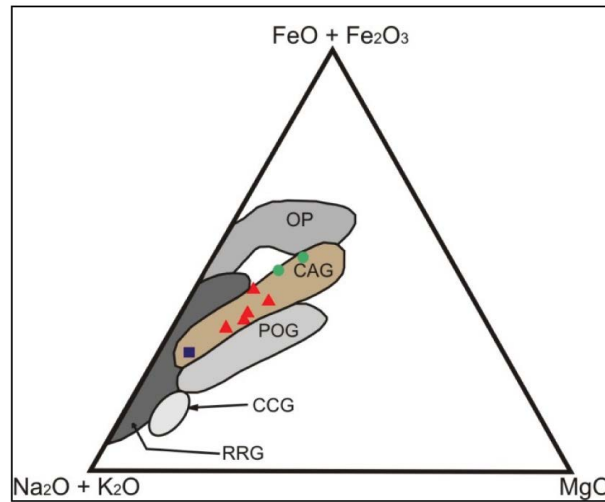


Figure 14. Location of the studied samples on the AFM diagram [33].

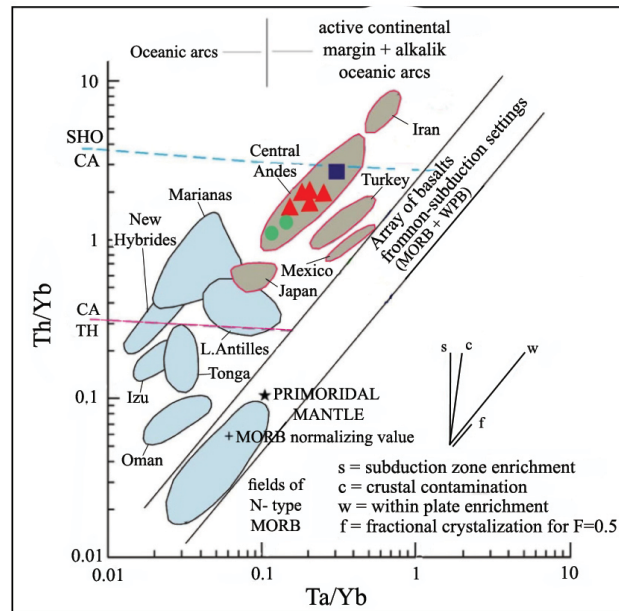


Figure 15. Location of the Neshveh intrusion sample on the Th/Yb versus Ta/Yb diagram [34].

As mentioned in the previous parts, based on [19] classification, Neshveh intrusion can be classified as ACG granitoids. According to him, ACG granitoids are hybrid type (mantle + crust) and are related with subduction settings. In this base, it is supposed a subduction setting to Neshveh intrusion.

7. Conclusion

Field studies, petrographic and geochemical investigations indicate that the Neshveh granitoid consists of the quartz-monzodiorite, granodiorite and granite. Field relations and geochemical studies demonstrate that all of these rocks are related to a single parent magma which underwent fractional crystallization. The Neshveh granitic intrusion has high-K calc-alkaline nature. This intrusion is metaluminous and classified as I-type granitoids. Negative anomalies of Nb and Ti along with positive anomalies of Rb, Ba, K, and Pb in the spider diagrams are indicative for the formation of this intrusion in relation with subduction setting. In terms of geodynamic setting, this intrusion is classified as volcanic arc granites (VAG) and active continental margin granites (CAG) which have been formed as a result of Neotethys oceanic crust subduction beneath the Central Iran continental crust.

Acknowledgements

This study was financially support by Research Deputy of Tehran University for the proposal entitled Petrography and Petrology of Neshveh intrusion (northwest Saveh). Our gratitude is expressed to their helps.

References

- [1] Caillat, C., Dehlavi, P. and Martel, J.B. (1978) Geologie de la region de Saveh (Iran). Contribution a l'etude du volcanism et du plutonism tertiares de la zone de I Iran central. PhD Thesis, Grenoble, 325 Pages.
- [2] Helmi, F. (1991) Petrology and geochemistry of igneous rocks in Niousht area (NE Saveh). M.Sc. Thesis, University of Tehran, Iran (in Persian).
- [3] Moinvaziri, H. (1999) Introduction to the Magmatism of Iran. Tarbiat Moallem University, Tehran (in Persian).
- [4] Galamgash, J. and Fonudi, M. (1998) Explanatory Text of Saveh. Geological Map 1:100,000. Geological Survey of Iran, Tehran.
- [5] Irvine, T.N. and Baragar, W.R.A. (1971) A Guide to Chemical Classification of the Common Volcanic Rock. *Canadian Journal of Earth Sciences*, **8**, 523-548. <http://dx.doi.org/10.1139/e71-055>
- [6] Kuno, H. (1968) Differentiation of Basalt Magmas. In: Hess, H.H. and Poldervaart, A., Eds., *Basalts: The Poldervaart Treatise on Rocks of Basaltic Composition*, Interscience Publishers, New York, 623-688.
- [7] Peccerillo, A. and Taylor, S.R. (1976) Geochemistry of Eocene Calc Alkaline Volcanic Rocks from Kastamonu Area, Northern Turkey. *Contribution to Mineralogy and Petrology*, **58**, 63-81. <http://dx.doi.org/10.1007/BF00384745>
- [8] Frost, B.F., Barnes, G.G., Collins, W.J., Arculus, R.J., Ellis, D.J. and Frost, C.D. (2001) A Geological Classification for Granitic Rocks. *Journal of Petrology*, **42**, 2033-2048. <http://dx.doi.org/10.1093/ptrology/42.11.2033>
- [9] Shand, S.J. (1943) *Eruptive Rocks*. 2nd Edition, John Wiley, New York.
- [10] Chappell, B.W. and White, A.J.R. (1974) Two Contrasting Granite Types. *Pacific Geology*, **8**, 173-174.
- [11] Collins, W.J., Beams, S.D., White, A.J.R. and Chappell, B.W. (1980) Nature and Origin of A-Type Granites with Particular Reference to South Eastern Australia. *Contribution to Mineralogy and Petrology*, **80**, 189-200. <http://dx.doi.org/10.1007/BF00374895>
- [12] Whalen, J.B., Currie, K.L. and Chappell, B.W. (1987) A-Type Granites: Geochemical Characteristics, Discrimination and Petrogenesis. *Contribution to Mineralogy and Petrology*, **95**, 407-419. <http://dx.doi.org/10.1007/BF00402202>
- [13] Castro, A., Monero-Venatas, I. and De La Rosa, J.D. (1991) H-Type (Hybrid) Granitoids: A Proposed Revision of the Granite Type Classification and Nomenclature. *Earth Science Reviews*, **31**, 237-253. [http://dx.doi.org/10.1016/0012-8252\(91\)90020-G](http://dx.doi.org/10.1016/0012-8252(91)90020-G)
- [14] Pitcher, W.S. (1993) *The Nature and Origin of Granite*. Blackie Academic and Professional Edition. Shopman and Hall, London. <http://dx.doi.org/10.1007/978-94-017-3393-9>
- [15] Chappell, B.W. and White, A.J.R. (2001) Two Contrasting Granite Types. 25 Years Later. *Australian Journal of Earth Sciences*, **48**, 489-499. <http://dx.doi.org/10.1046/j.1440-0952.2001.00882.x>
- [16] Didier, J., Duthou, J.L. and Lameyre, J. (1982) Mantle and Crustal Granites: Genetic Classification of Orogenic Granites and the Nature of Their Enclaves. *Journal of Volcanology and Geothermal Research*, **14**, 125-132. [http://dx.doi.org/10.1016/0377-0273\(82\)90045-2](http://dx.doi.org/10.1016/0377-0273(82)90045-2)

- [17] Chappell, B.W. and White, A.J.R. (1992) I- and S-Type Granites in the Lachlan Fold Belt. *Transactions of the Royal Society of Edinburgh: Earth Sciences*, **83**, 1-26. <http://dx.doi.org/10.1017/S0263593300007720>
- [18] Chappell, B.W. and White, A.J.R. (1983) Granitoid Types and Their Distribution in the Lachlan Fold Belt, Southeastern Australia. *Geological Society of America Memoirs*, **159**, 21-34. <http://dx.doi.org/10.1130/MEM159-p21>
- [19] Barbarin, B. (1999) A Review of the Relationships between Granitoid Types, Their Origins and Their Geodynamic Environments. *Lithos*, **46**, 605-626. [http://dx.doi.org/10.1016/S0024-4937\(98\)00085-1](http://dx.doi.org/10.1016/S0024-4937(98)00085-1)
- [20] Bourdon, E., Eissen, J.P., Monzier, M., Rovin, C., Martin, H., Cotten, J. and Hall, M.L. (2002) Adakite-Like Lavas from Antisana Volcano (Ecuador): Evidence for Slab Melt Metasomatism beneath the Andean Northern Volcanic Zone. *Journal of Petrology*, **43**, 199-217. <http://dx.doi.org/10.1093/petrology/43.2.199>
- [21] Cocherie, A. (1986) Systematic Use of Trace Element Distribution on Patterns in Log-Log Diagrams for Plutonic Suites. *Geochimica et Cosmochimica Acta*, **50**, 2517-2522. [http://dx.doi.org/10.1016/0016-7037\(86\)90034-7](http://dx.doi.org/10.1016/0016-7037(86)90034-7)
- [22] Woodhead, J.D. and Johnson, R.W. (1993) Isotopic and Trace Element Profile across the New Britain Island Arc, Papua New Guinea. *Contributions to Mineralogy and Petrology*, **113**, 479-491. <http://dx.doi.org/10.1007/BF00698317>
- [23] Sun, S.S. and McDonough, W.F. (1989) Chemical and Isotopic Systematics of Oceanic Basalts: Implications for Mantle Composition and Processes. In: Saunders, A.D. and Norry, M.J., Eds., *Magmatism in the Ocean Basins*, Vol. 42, Geological Society Special Publication, London, 313-345.
- [24] Glenn, A.G. (2004) The Influence of Melt Structure on Trace Element Partitioning near the Peridotite Solidus. *Contributions to Mineralogy and Petrology*, **147**, 511-527. <http://dx.doi.org/10.1007/s00410-004-0575-1>
- [25] Wilson, M. (2007) *Igneous Petrogenesis*. Chapman and Hall, London.
- [26] Sajona, F.G., Maury, R.C., Bellon, H., Cotton, J. and Defant, M. (1996) High Field Strength Elements Enrichment of Pliocene-Pleistocene Island Arc Basalts Zamboanga Peninsula, Western Mindanao (Philippines). *Journal of Petrology*, **37**, 693-726. <http://dx.doi.org/10.1093/petrology/37.3.693>
- [27] Chappell, B.W. (1999) Aluminium Saturation in I- and S-Type Granites and the Characterization of Fractionated Haplogranites. *Lithos*, **46**, 535-551. [http://dx.doi.org/10.1016/S0024-4937\(98\)00086-3](http://dx.doi.org/10.1016/S0024-4937(98)00086-3)
- [28] Kamber, B.S., Ewart, A., Collerson, K.D., Bruce, M.C. and McDonald, G.D. (2002) Fluid-Mobile Trace Element Constraints on the Role of Slab Melting and Implications for Archean Crustal Growth Models. *Contributions to Mineralogy and Petrology*, **144**, 38-56. <http://dx.doi.org/10.1007/s00410-002-0374-5>
- [29] Atherton, M.P. and Ghani, A.A. (2002) Slab Breakoff: A Model for Caledonian, Late Granite Syncollisional Magmatism in the Orthotectonic (Metamorphic) Zone of Scotland and Donegal, Ireland. *Lithos*, **62**, 65-85. [http://dx.doi.org/10.1016/S0024-4937\(02\)00111-1](http://dx.doi.org/10.1016/S0024-4937(02)00111-1)
- [30] Batchelor, R.A. and Bowden, P. (1985) Petrogenetic Interpretation of Granitoid Rock Series Using Multicationic Parameters. *Chemical Geology*, **48**, 43-55. [http://dx.doi.org/10.1016/0009-2541\(85\)90034-8](http://dx.doi.org/10.1016/0009-2541(85)90034-8)
- [31] Harris, N.B.W., Pearce, J.A. and Tindle, A.G. (1986) Geochemical Characteristics of Collision Zone Magmatism. *Collision Tectonic, Geological Society of American Bulletin*, Special Publication, **19**, 67-81. <http://dx.doi.org/10.1144/GSL.SP.1986.019.01.04>
- [32] Pearce, J.A. (1996) Sources and Settings of Granitic Rocks. *Episodes*, **19**, 120-125.
- [33] Gorton, M.P. and Schandl, E.S. (2002) From Continents to Island Arc: A Geochemical Index of Tectonic Setting for Arc-Related and within Plate Felsic to Intermediate Volcanic Rocks. *Canadian Mineralogist*, **38**, 1065-1073. <http://dx.doi.org/10.2113/gscanmin.38.5.1065>
- [34] Bowden, P., Batchelor, R.A., Chappelle, B.W., Didier, J. and Lameyer, J. (1984) Petrological, Geochemical and Source Criteria for the Classification of Granitic Rocks: A Discussion. *Physics of the Earth and Planetary Interiors*, **35**, 1-11. [http://dx.doi.org/10.1016/0031-9201\(84\)90029-3](http://dx.doi.org/10.1016/0031-9201(84)90029-3)
- [35] Pearce, J.A., Harris, N.B.W. and Tindle, A.G. (1984) Trace Element Discrimination Diagrams for the Tectonic Interpretation of Granitic Rocks. *Journal of Petrology*, **25**, 956-983. <http://dx.doi.org/10.1093/petrology/25.4.956>